

# GCEPNet: Graph Convolution-Enhanced Expectation Propagation for Massive MIMO Detection

Qincheng Lu

*School of Computer Science  
McGill University  
Montreal, Canada  
qincheng.lu@mail.mcgill.ca*

Sitao Luan

*McGill University  
Mila - Quebec AI Institute  
Montreal, Canada  
sitao.luan@mail.mcgill.ca*

Xiao-Wen Chang

*School of Computer Science  
McGill University  
Montreal, Canada  
chang@cs.mcgill.ca*

**Abstract**—Massive MIMO (multiple-input multiple-output) detection is an important topic in wireless communication and various machine learning based methods have been developed recently for this task. Expectation Propagation (EP) and its variants are widely used for MIMO detection and have achieved the best performance. However, EP-based solvers fail to capture the correlation between unknown variables, leading to a loss of information, and in addition, they are computationally expensive. In this paper, we show that the real-valued system can be modeled as spectral signal convolution on graph, through which the correlation between unknown variables can be captured. Based on such analysis, we propose graph convolution-enhanced expectation propagation (GCEPNet). GCEPNet incorporates data-dependent attention scores into Chebyshev polynomial for powerful graph convolution with better generalization capacity. It enables a better estimation of the cavity distribution for EP and empirically achieves the state-of-the-art (SOTA) MIMO detection performance with much faster inference speed. To our knowledge, we are the first to shed light on the connection between the system model and graph convolution, and the first to design the data-dependent coefficients for graph convolution.

**Index Terms**—massive MIMO detection, machine learning for communication, graph convolution, expectation propagation

## I. INTRODUCTION

Massive MIMO (multiple-input multiple-output) is a wireless communication technology that uses a very large number of antennas at the base station to significantly increase spectral efficiency and capacity [1]. One of the outstanding challenges in massive MIMO is to efficiently detect the transmitted signal. Finding the optimal detector can be modeled as solving an integer least square problem, which is NP-hard [2]. As the complexity of the traditional methods for near-optimal solutions still grows prohibitively as the number of users increases, especially for large-scale problem, methods inspired by deep learning have emerged as promising solutions to meet the high throughput and low latency requirements [3]. Achieving a comparable detection performance to the traditional methods, the learning-based methods shift the significant part of computational cost to an offline training phase and significantly shorten run time in the online detection (inference) phase [4].

For improving the performance of conventional detectors [5]–[10], various machine learning methods for MIMO detection have been proposed [4], including pure learning-based methods [11], [12], and the methods which incorporate learnable parameters [13]–[15] or learnable modules [16]–[19] into some conventional detectors. Among them, graph neural network (GNN) aided message passing (MP) detectors [16]–[19] stands out with better performance. In GNN aided MP detectors, GNN is used to improve the approximation of posterior distribution in various MP detectors, including Expectation Propagation (EP) [9], Approximate Message Passing (AMP) [10] and Bayesian parallel interference cancellation (BPIC) [20]. The GNN aided EP framework (GEPNet) [16] and its variant IEP-GNN [19] (to be elaborated later) achieve the best performance among well-known conventional sub-optimal detectors and those which apply machine learning techniques.

Here is a brief history about the incorporation of GNNs into MP. GEPNet is the pioneering work, but its computation involves matrix inversion due to the EP iterations [16]. As it is inefficient, later efforts were made to leverage other MP methods in GEPNet. For example, GPICNet [17] substitutes the EP module with BPIC, and AMP-GNN [18] replaces it by AMP. Although both changes reduce complexity, they degrade GEPNet’s performance. Very recently, IEP-GNN [19] was proposed to improve the computation of local posterior information in the EP iteration, which enhances the performance of GEPNet while maintaining the same computational cost. However, to our best knowledge, there is no existing work that aims to improve the efficiency of the GNN module in GEPNet. In this paper, we focus on addressing the inefficiency issue of the GNN module in GEPNet, with no performance degradation and sometimes even performance enhancement. The proposed method can be seamlessly integrated with IEP-GNN.

Meanwhile, the theoretical justification, expressivity, and efficiency of the currently widely adopted GNNs framework for MIMO detection are under-explored. For example, existing GNNs for MIMO are intuitively based on the pairwise Markov Random Field (MRF) factorization of the posterior [11], [16], [17], where a spatial GNN is utilized to

parameterize and learn the representation of the variable and factor nodes in the MRF model. However, the formulation of these GNNs inherits from works that combine deep learning with MRF [11], but less motivated by the unique property of MIMO detection problem. In addition, spatial GNNs originate as the low order approximation of the graph convolution [21], which loses high-order topology information. To enhance the expressivity of the MIMO-specific GNNs, we investigate the connection between the system model and the graph convolution, and propose a novel graph convolution-enhanced EP detector (GCEPNet)<sup>1</sup>, which achieves state-of-the-art detection performance with fewer training parameters and lower inference complexity.

The rest of the paper is organized as follows. Section II gives notation and reviews spectral graph convolution. Section III introduces the MIMO system model. The machine learning approach for MIMO detection is outlined in Section IV. Section V presents the use of GNN in the EP detector. We propose the GCEPNet in Section VI and show its efficiency in Section VII. Section VIII provides training details and performance comparison. Section IX concludes the paper.

## II. PRELIMINARIES

### A. Notation

We use bold capital and small letters for matrices and vectors, respectively. The  $(i, j)$  entry of  $\mathbf{A}$  is denoted by  $\mathbf{A}(i, j)$  or  $a_{ij}$ , the  $i^{th}$  row of  $\mathbf{A}$  is denoted by  $\mathbf{A}_{i,:}$ , and the  $i^{th}$  entry of  $\mathbf{s}$  is denoted by  $\mathbf{s}(i)$  or  $s_i$ . We denote  $\mathbf{1} = [1, \dots, 1]^\top$ . When a real-valued random vector  $\mathbf{x}$  follows the normal distribution with mean  $\boldsymbol{\mu}$  and covariance matrix  $\boldsymbol{\Sigma}$ , we write  $\mathbf{x} \sim \mathcal{N}(\boldsymbol{\mu}, \boldsymbol{\Sigma})$  and use  $N(\mathbf{x} : \boldsymbol{\mu}, \boldsymbol{\Sigma})$  to denote its density function.

### B. Graph and Convolution

For a graph  $\mathcal{G} = (\mathcal{V}, \mathcal{E})$ , where  $\mathcal{V}$  is the vertex set with  $N$  vertices (or nodes), *i.e.*,  $|\mathcal{V}| = N$ , and  $\mathcal{E}$  is the set of edges, the adjacency matrix of  $\mathcal{G}$  is defined as  $\mathbf{A} \in \mathbb{R}^{N \times N}$  with  $a_{ij} = 1$  if  $e_{ij} \in \mathcal{E}$  and  $a_{ij} = 0$  otherwise. The degree matrix is denoted as  $\mathbf{D} = \text{diag}(d_{ii}) \in \mathbb{R}^{N \times N}$  with  $d_{ii} = \sum_j a_{ij}$ . There are various graph Laplacians in the literature [22], [23], and among them, the symmetric normalized graph Laplacian is most widely used one  $\mathbf{L} = \mathbf{I} - \mathbf{D}^{-\frac{1}{2}} \mathbf{A} \mathbf{D}^{-\frac{1}{2}}$ . Let its eigen-decomposition be  $\mathbf{L} = \mathbf{U} \boldsymbol{\Lambda} \mathbf{U}^\top$ , where  $\boldsymbol{\Lambda} = \text{diag}(\lambda_i)$  with  $0 = \lambda_1 < \lambda_2 \leq \dots \leq \lambda_N \leq 2$  and  $\mathbf{U}$  is orthogonal. Given a graph signal  $\mathbf{s} \in \mathbb{R}^N$ , the graph Fourier transform and the inverse graph Fourier transform are defined as

$$\hat{\mathbf{s}} := \mathcal{F}(\mathbf{s}) := \mathbf{U}^\top \mathbf{s}, \quad \mathbf{s} := \mathcal{F}^{-1}(\hat{\mathbf{s}}) := \mathbf{U} \hat{\mathbf{s}}, \quad (1)$$

respectively. The graph convolution between graph signals  $\mathbf{s}_1 \in \mathbb{R}^N$  and  $\mathbf{s}_2 \in \mathbb{R}^N$  is defined as (see, *e.g.*, [21])

$$\mathbf{s}_2 *_{\mathcal{G}} \mathbf{s}_1 := \mathcal{F}^{-1}(\mathcal{F}(\mathbf{s}_2) \odot \mathcal{F}(\mathbf{s}_1)) = \mathbf{U}(\mathbf{U}^\top \mathbf{s}_2 \odot \mathbf{U}^\top \mathbf{s}_1), \quad (2)$$

where  $\odot$  is an element-wise multiplication operation.

### C. Spectral graph convolution

We briefly review the spectral graph convolution for graph signal processing and ChebNet [21], which will be used later. Suppose a function  $g_\theta$  which operates on the eigenvalues of the graph Laplacian  $\mathbf{L}$  is defined as  $\mathbf{g}_\theta(\lambda(\mathbf{L})) := [g_\theta(\lambda_1), \dots, g_\theta(\lambda_N)]^\top$ . The graph spectral filter associated with  $\mathbf{g}_\theta(\lambda(\mathbf{L}))$  is a linear operator  $\mathbf{T}_{g_\theta} : \mathbb{R}^N \rightarrow \mathbb{R}^N$  satisfying

$$\mathbf{T}_{g_\theta} \mathbf{s} = \mathcal{F}^{-1}(\mathbf{g}_\theta(\lambda(\mathbf{L})) \odot \mathcal{F}(\mathbf{s})) = \mathbf{U} \text{diag}(\mathbf{g}_\theta(\lambda(\mathbf{L}))) \mathbf{U}^\top \mathbf{s}. \quad (3)$$

Various designs of  $g_\theta(\lambda)$  lead to different spectral graph convolutions. It is proved that any graph convolution with well-defined analytic spectral filter can be written in a truncated block Krylov form [24] and polynomial filter is one of the most commonly used instances. For a polynomial  $g_\theta(\lambda) = \sum_{m=0}^M c_m \lambda^m$ , the graph convolution in (3) becomes

$$\mathbf{T}_{g_\theta} \mathbf{s} = \mathbf{U} \left( \sum_{m=0}^M c_m \boldsymbol{\Lambda}^m \right) \mathbf{U}^\top \mathbf{s} = \sum_{m=0}^M c_m \mathbf{L}^m \mathbf{s}. \quad (4)$$

In [21], ChebNet is proposed to use Chebyshev polynomials to fit (4) as

$$\mathbf{T}_{g_\theta} \mathbf{s} = \sum_{m=0}^M w_m T_m(\hat{\mathbf{L}}) \mathbf{s}, \quad (5)$$

where  $T_m(x)$  are Chebyshev polynomials defined by  $T_m(x) = 2xT_{m-1}(x) - T_{m-2}(x)$ ,  $T_0(x) = 1$  and  $T_1(x) = x$ .

## III. SYSTEM MODEL

Suppose that in a MIMO system, the transmitter is equipped with  $N_t$  antennas and the receiver is equipped with  $N_r$  antennas, and the transmitted signal  $\mathbf{x}_c$  and the received signal  $\mathbf{y}_c$  satisfy the following model:

$$\mathbf{y}_c = \mathbf{H}_c \mathbf{x}_c + \mathbf{n}_c, \quad (6)$$

where the channel matrix  $\mathbf{H}_c \in \mathbb{C}^{N_r \times N_t}$  is assumed to be known to the receiver; the elements of  $\mathbf{x}_c \in \mathcal{X}_c^{N_t}$  are independently distributed over the constellation set  $\mathcal{X}_k = \{k_1 + k_2 j : k_1, k_2 = \pm 1, \pm 3, \dots, \pm (2^k - 3), \pm (2^k - 1)\}$ ,  $k = 1, 2, 3$  correspond to QPSK, *i.e.*, 4QAM, 16QAM, 64QAM constellations, respectively; and the complex circular Gaussian noise  $\mathbf{n}_c \sim \mathcal{CN}(\mathbf{0}, \sigma_c^2 \mathbf{I})$ . Given  $\mathbf{y}_c$  and  $\mathbf{H}_c$ , our objective is to estimate  $\mathbf{x}_c$ . Define

$$\mathbf{y} = \begin{bmatrix} \mathcal{R}(\mathbf{y}_c) \\ \mathcal{I}(\mathbf{y}_c) \end{bmatrix}, \quad \mathbf{H} = \begin{bmatrix} \mathcal{R}(\mathbf{H}_c) & -\mathcal{I}(\mathbf{H}_c) \\ \mathcal{I}(\mathbf{H}_c) & \mathcal{R}(\mathbf{H}_c) \end{bmatrix}, \quad \mathbf{x} = \begin{bmatrix} \mathcal{R}(\mathbf{x}_c) \\ \mathcal{I}(\mathbf{x}_c) \end{bmatrix}, \quad \mathbf{n} = \begin{bmatrix} \mathcal{R}(\mathbf{n}_c) \\ \mathcal{I}(\mathbf{n}_c) \end{bmatrix}, \quad \mathcal{X}_k = \{\pm 1, \dots, \pm (2^k - 1)\}, \quad (7)$$

where  $\mathcal{R}(\cdot)$  and  $\mathcal{I}(\cdot)$  denote the real and imaginary parts. Then the complex system model in (6) becomes

$$\mathbf{y} = \mathbf{H}\mathbf{x} + \mathbf{n}, \quad \mathbf{n} \sim \mathcal{N}(\mathbf{0}, \sigma_n^2 \mathbf{I}). \quad (8)$$

where  $\mathbf{x} \in \mathcal{X}_k^{2N_t}$ ,  $\mathbf{H} \in \mathbb{R}^{2N_r \times 2N_t}$ ,  $\sigma_n^2 = \sigma_c^2/2$ . The maximum likelihood method for detecting  $\mathbf{x}$  in (8) solves the integer least squares (ILS) problem:

$$\min_{\mathbf{x} \in \mathcal{X}_k^{2N_t}} \|\mathbf{y} - \mathbf{H}\mathbf{x}\|_2^2. \quad (9)$$

<sup>1</sup>Code available at: <https://github.com/wzzlcss/GCEPNet>

In this paper we assume that  $\mathbf{H}$  has full column rank. This is usually true in practice. As (9) is NP-hard, the maximum likelihood detection for a large MIMO system is prohibited.

#### IV. MACHINE LEARNING FOR MIMO DETECTION

From the machine learning perspective, MIMO detection can be regarded as a classification problem, where we classify each component of the unknown  $\mathbf{x}$  in (8) into  $2^k$  categories defined by the constellation set  $\mathcal{X}_k$ . For convenience, we abuse the notation and regard  $\mathcal{X}_k$  as a tuple, and order its  $2^k$  elements, with the  $j^{th}$  element denoted by  $\mathcal{X}_k(j)$ . Then, our goal is to learn a function  $\mathbf{f}_\theta : \mathbf{y}, \mathbf{H} \rightarrow \mathbf{Z} \in \mathbb{R}^{2N_t \times 2^k}$ , where  $\mathbf{Z}(i, j)$  is proportional to the probability of  $x_i$  being labeled as  $\mathcal{X}_k(j)$ . And  $\theta$  is a vector of trainable parameters of the network, which is to be optimized by minimizing a loss function with training data samples. In application,  $\mathbf{f}_\theta$  computes the soft estimation  $\hat{a}_i$  of  $x_i$  and its variance  $\hat{b}_i^2$ :

$$\Pr(x_i = \mathcal{X}_k(j)|\mathbf{y}, \mathbf{H}) = \frac{\exp\{\mathbf{Z}(i, j)\}}{\sum_\ell \exp\{\mathbf{Z}(i, \ell)\}}, \quad (10)$$

$$\hat{a}_i = \sum_j \mathcal{X}_k(j) \times \Pr(x_i = \mathcal{X}_k(j)|\mathbf{y}, \mathbf{H}), \quad (11)$$

$$\hat{b}_i^2 = \sum_j (\mathcal{X}_k(j) - \hat{a}_i)^2 \times \Pr(x_i = \mathcal{X}_k(j)|\mathbf{y}, \mathbf{H}) \quad (12)$$

where (10) is referred to as the softmax normalization of the  $i^{th}$  row of  $\mathbf{Z}$ . A component-wise hard decision is obtained by rounding each element of  $\hat{a}_i$  independently onto the constellation set:

$$\hat{x}_i = \operatorname{argmin}_{x \in \mathcal{X}_k} |x - \hat{a}_i|. \quad (13)$$

#### V. GNN-AIDED EXPECTATION PROPAGATION

We briefly introduce the EP detector and explain the use of GNN in EP. For the system model defined in (8), the posterior probability density of  $\mathbf{x}$  is given by Bayes' rule:

$$p(\mathbf{x}|\mathbf{y}, \mathbf{H}) \propto p(\mathbf{y}|\mathbf{x}, \mathbf{H})p(\mathbf{x}) = N(\mathbf{y} : \mathbf{H}\mathbf{x}, \sigma_n^2 \mathbf{I}) \prod_{i=1}^{2N_t} p(x_i), \quad (14)$$

where the prior  $p(x_i) = \mathbb{1}_{x_i \in \mathcal{X}_k}$ , which is an indicator function. The EP detector tries to find an approximate Gaussian distribution  $q(\mathbf{x}|\mathbf{y}, \mathbf{H}) = N(\mathbf{x} : \boldsymbol{\mu}_\mathbf{x}, \boldsymbol{\Sigma}_\mathbf{x})$  to estimate the intractable  $p(\mathbf{x}|\mathbf{y}, \mathbf{H})$ , and then rounds  $\boldsymbol{\mu}_\mathbf{x}$  to the nearest integer point in the constellation set  $\mathcal{X}_k^n$  to get the estimation of  $\mathbf{x}$  in (8). To this end, we need first to find out a suitable prior  $p(x_i)$ , and the EP detector replaces the non-Gaussian prior in (14) with unnormalized Gaussian distribution as follows,

$$\prod_{i=1}^{2N_t} p(x_i) \approx \prod_{i=1}^{2N_t} g(x_i) := \prod_{i=1}^{2N_t} \exp\left\{-\frac{1}{2}\theta_{ii}x_i^2 + \gamma_i x_i\right\} \quad (15)$$

$$= \exp\left\{-\frac{1}{2}\mathbf{x}^\top \boldsymbol{\Theta} \mathbf{x} + \mathbf{x}^\top \boldsymbol{\gamma}\right\}, \quad (16)$$

where  $\boldsymbol{\Theta} = \operatorname{diag}(\theta_{ii})$  and  $\boldsymbol{\gamma} = (\gamma_i)$ . The EP detector finds  $\boldsymbol{\Theta}$  and  $\boldsymbol{\gamma}$  through iterative methods [9]. At the  $t^{th}$  iteration, the posterior approximation  $p^{(t)}(\mathbf{x}|\mathbf{y}, \mathbf{H})$  is given by

$$\begin{aligned} p^{(t)}(\mathbf{x}|\mathbf{y}, \mathbf{H}) &= N(\mathbf{x} : \boldsymbol{\mu}_\mathbf{x}^{(t)}, \boldsymbol{\Sigma}_\mathbf{x}^{(t)}) \\ &\propto N(\mathbf{y} : \mathbf{H}\mathbf{x}, \sigma_n^2 \mathbf{I}) \exp\left\{-\frac{1}{2}\mathbf{x}^\top \boldsymbol{\Theta}^{(t-1)} \mathbf{x} + \mathbf{x}^\top \boldsymbol{\gamma}^{(t-1)}\right\}. \end{aligned}$$

We can take  $\boldsymbol{\Theta}^{(0)} = \operatorname{cov}\{\mathbf{x}\} = \sigma_\mathbf{x}^{-2} \mathbf{I}$  (suppose  $\sigma_\mathbf{x}$  is known) and  $\boldsymbol{\gamma}^{(0)} = \mathbf{0}$ . Denote the  $i^{th}$  marginal of  $p^{(t)}(\mathbf{x}|\mathbf{y}, \mathbf{H})$  as

$$q^{(t)}(x_i|\mathbf{y}, \mathbf{H}) = N(\boldsymbol{\mu}_\mathbf{x}^{(t)}(i), \boldsymbol{\Sigma}_\mathbf{x}^{(t)}(i, i)). \quad (17)$$

At each iteration, an improved posterior  $\hat{p}^{(t)}(x_i)$  of  $x_i$  can be obtained by replacing the approximation factor  $g(x_i)$  from  $q^{(t)}(x_i|\mathbf{y}, \mathbf{H})$  by the true factor  $p(x_i) = \mathbb{1}_{x_i \in \mathcal{X}_k}$  [9]:

$$q^{(t)\setminus i}(x_i) := \frac{q^{(t)}(x_i|\mathbf{y}, \mathbf{H})}{\exp\left\{-\frac{1}{2}\theta_{ii}^{(t-1)}x_i^2 + \gamma_i^{(t-1)}x_i\right\}}, \quad (18)$$

$$\hat{p}^{(t)}(x_i) \propto q^{(t)\setminus i}(x_i) \mathbb{1}_{x_i \in \mathcal{X}_k}. \quad (19)$$

From (18) and (19), the EP detector finds the cavity distribution  $q^{(t)\setminus i}(x_i) = N(x_i : a_i^{(t)}, (b_i^{(t)})^2)$  and  $\hat{p}^{(t)}(x_i) = N(x_i : \hat{\mu}_i^{(t)}, (\hat{\sigma}_i^{(t)})^2)$  as shown in [9]. Then the EP detector finds  $\theta_{ii}^{(t)}$  and  $\gamma_i^{(t)}$  satisfying

$$N(\hat{\mu}_i^{(t)}, \hat{\sigma}_i^{(t)2}) \propto q^{(t)\setminus i}(x_i) \exp\left\{-\frac{1}{2}\theta_{ii}^{(t)}x_i^2 + \gamma_i^{(t)}x_i\right\}. \quad (20)$$

Although the EP detector has been shown to outperform various conventional sub-optimal detectors across different problem sizes and QAM orders [9], it only uses the local Gaussian distribution (17) to define the cavity distribution in (18), which treats each element in  $\mathbf{x}$  independently. Such assumption of independence is strong, ignoring the correlation information in the off-diagonal elements of  $\boldsymbol{\Sigma}_\mathbf{x}^{(t)}$ , and thus failing to capture the synergy between the components of  $\mathbf{x}$ . To deal with this issue, GEPNet uses a graph neural network to model the such correlations and learn  $N(\hat{\mu}_i^{(t)}, (\hat{b}_i^{(t)})^2)$  via (10), (11), (12) to replace the  $q^{(t)\setminus i}(x_i)$  in (19) at the  $t^{th}$  EP iteration, and use  $\hat{a}_i^{(T)}$  at the last EP iteration ( $t = T$ ) to give the final detection in (13). More details about GEPNet will be given in Section VII.

#### VI. EFFICIENT GRAPH CONVOLUTION-BASED MIMO DETECTOR

In this section, we propose the graph convolution-enhanced expectation propagation (GCEPNet), a novel graph neural network architecture with theoretical support that provides an efficient scheme to incorporate correlations among unknown symbols for MIMO detection. The proposed method effectively addresses not only the limitation of the loss of correlation information in the original EP detector but also the computation bottleneck in the existing state-of-the-art GNNs for MIMO, and lays the foundation for designing better graph convolution neural networks for MIMO detection in future research.

##### A. The Graph Convolution Form of the System Model

In this section, we show that the system model can be described by a graph convolution. In order to learn the representation of unknown  $x_i$  as well as the correlations among them, for each instance, we define a fully connected self-loop graph  $\mathcal{G}_{\text{MIMO}} = (\mathcal{V}_\mathbf{x}, \mathcal{E}_\mathbf{x})$  with node  $i \in \mathcal{V}_\mathbf{x}$  representing  $x_i$  from the problem instance. In  $\mathcal{G}_{\text{MIMO}}$ , there exists edge  $e_{ij}$  between each pair of nodes  $(i, j)$ , indicating the potential

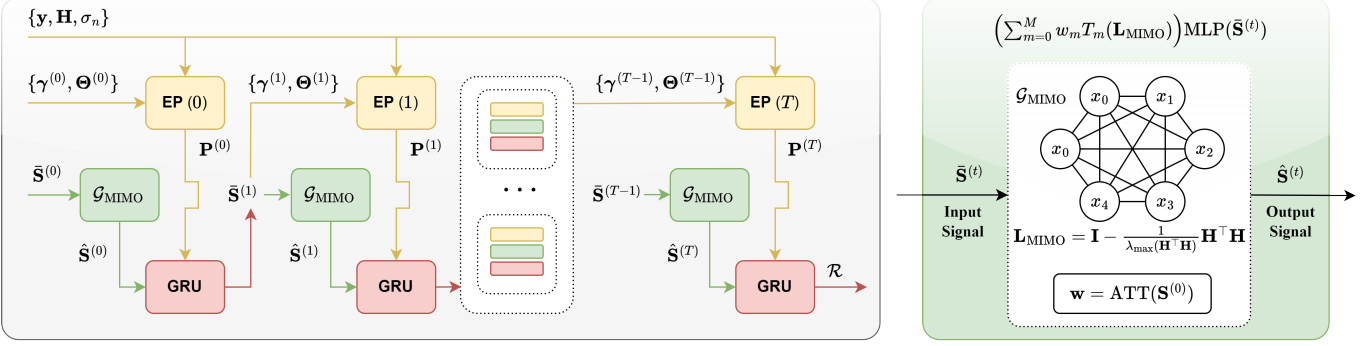


Fig. 1. The structure of GCEPNet. The left panel shows the main workflow, where an iteration  $t$  contains three modules that perform EP calculation, graph convolution and GRU gating respectively. Arrows indicate the data flow. The right panel illustrates the graph convolution process, that computes (27) and (28), using  $N_t = 3$  as an example.

correlations. The available  $\mathbf{y}$ ,  $\mathbf{H}$  and  $\sigma_n$  of the instance are encoded in the Laplacian and graph signal on  $\mathcal{G}_{\text{MIMO}}$ . We define a normalized graph Laplacian of  $\mathcal{G}_{\text{MIMO}}$  as

$$\mathbf{L}_{\text{MIMO}} = \mathbf{I} - \alpha \mathbf{H}^T \mathbf{H} := \mathbf{I} - \mathbf{W}, \quad \alpha := 1/\lambda_{\max}(\mathbf{H}^T \mathbf{H}), \quad (21)$$

where  $\mathbf{W} = \alpha \mathbf{H}^T \mathbf{H}$  is a weight matrix of the graph and  $\mathbf{W}(i, j)$  is a weight for the edge  $e_{ij}$ . Like different variants of the graph Laplacian [23],  $\mathbf{L}_{\text{MIMO}}$  has nonnegative eigenvalues, more specifically,  $\lambda(\mathbf{L}_{\text{MIMO}}) \in [0, 1]$ . Note that the weights  $\mathbf{W}(i, j)$  can be negative for  $i \neq j$ , and for self-loop edges,  $\mathbf{W}(i, i)$  are not all equal. Thus,  $\mathbf{L}_{\text{MIMO}}$  has some differences with the existing graph Laplacian and can be regarded as an extension of it.

Since in the real-valued system model in equation (8)  $\mathbf{H}$  is assumed to have full column rank, multiplying both sides of equation (8) by  $(\mathbf{H}^T \mathbf{H})^{-1} \mathbf{H}^T$  gives

$$\mathbf{x} = (\mathbf{H}^T \mathbf{H})^{-1} (\mathbf{H}^T \mathbf{y} + \mathbf{H}^T \mathbf{n}) = (\alpha \mathbf{H}^T \mathbf{H})^{-1} (\alpha \mathbf{H}^T \mathbf{y} + \alpha \mathbf{H}^T \mathbf{n}). \quad (22)$$

Since  $|\lambda(\mathbf{L}_{\text{MIMO}})| < 1$ ,

$$(\alpha \mathbf{H}^T \mathbf{H})^{-1} = (\mathbf{I} - \mathbf{L}_{\text{MIMO}})^{-1} = \sum_{m=0}^{\infty} \mathbf{L}_{\text{MIMO}}^m.$$

Then from (22) we obtain

$$\mathbf{x} = \left( \sum_{m=0}^{\infty} \mathbf{L}_{\text{MIMO}}^m \right) (\alpha \mathbf{H}^T \mathbf{y} + \alpha \mathbf{H}^T \mathbf{n}). \quad (23)$$

This shows that the real-valued system can be modeled as spectral signal convolution on graph, where we have  $2N_t$  nodes and weight matrix  $\mathbf{W}$ . More specifically,  $\mathbf{x}$  can be regarded as the graph convolution between the polynomial filter  $\mathbf{g}(\lambda(\mathbf{L}_{\text{MIMO}})) = \sum_{m=0}^{\infty} \lambda(\mathbf{L}_{\text{MIMO}})^m$  and the graph signal  $\alpha \mathbf{H}^T \mathbf{y} + \alpha \mathbf{H}^T \mathbf{n}$  as shown in equation (4). Therefore, a graph convolution-based GNN could be employed to learn the deep representations for each unknown  $x_i$  in the system model.

### B. Architecture of GCEPNet

Based on the discussion in previous sections, we propose a graph convolution-based method, GCEPNet, to improve the estimation of cavity distribution in (19) with faster inference,

which would later be used in the EP iteration. According to (23), we initialize the input graph signal  $\mathbf{S}^{(0)} \in \mathbb{R}^{2N_t \times 2}$  as

$$\mathbf{S}^{(0)} = [\alpha \mathbf{H}^T \mathbf{y}, \alpha \sigma_n \mathbf{H}^T \mathbf{1}], \quad (24)$$

where  $\alpha \sigma_n \mathbf{H}^T \mathbf{1}$  is used to approximate the unknown  $\alpha \mathbf{H}^T \mathbf{n}$  in (23), and the  $i$ -th row of  $\mathbf{S}^{(0)}$  is a graph signal of the node  $i$  corresponding to  $x_i$ . The key operation in GCEPNet is that we use the graph convolution in equation (23) to recover useful information about the unknown  $\mathbf{x}$  from the graph signal defined in (24), by the following approximated Chebyshev polynomials with order  $M$ ,

$$\sum_{m=0}^{\infty} (\mathbf{L}_{\text{MIMO}})^m \approx \sum_{m=0}^M w_m T_m(\mathbf{L}_{\text{MIMO}}). \quad (25)$$

At  $t^{th}$  EP iteration, based on the cavity density of each  $x_i$  in (18), we construct  $\mathbf{a}^{(t)} = [a_0^{(t)}, \dots, a_{2N_t}^{(t)}]^T$ ,  $\mathbf{b}^{(t)} = [(b_0^{(t)})^2, \dots, (b_{2N_t}^{(t)})^2]^T$ , and denote  $\mathbf{P}^{(t)} = [\mathbf{a}^{(t)}, \mathbf{b}^{(t)}]$ , where  $\mathbf{P}^{(t)}$  contains the mean and variance information for  $x_i$ . GCEPNet intends to improve the standard cavity density by incorporating pair-wise information learned via the graph convolution on  $\mathcal{G}_{\text{MIMO}}$  efficiently. In Figure 1, we present the overall structure of GCEPNet. For  $t = 0 \dots T$ ,

$$\bar{\mathbf{S}}^{(0)} = \mathbf{S}^{(0)} \mathbf{W}_0 + \mathbf{B}_0, \quad (26)$$

$$\tilde{\mathbf{S}}^{(t)} = \text{MLP}_1(\bar{\mathbf{S}}^{(t)}), \quad (27)$$

$$\hat{\mathbf{S}}^{(t)} = \sum_{m=0}^M \text{ATT}(\mathbf{S}^{(0)})_m T_m(\mathbf{L}_{\text{MIMO}}) \tilde{\mathbf{S}}^{(t)}, \quad (28)$$

$$\bar{\mathbf{S}}^{(t+1)} = \text{GRU}(\hat{\mathbf{S}}^{(t)}, \mathbf{P}^{(t)}), \quad (29)$$

$$\mathbf{P}_G^{(t)} = R(\text{MLP}_2(\bar{\mathbf{S}}^{(t+1)})). \quad (30)$$

Equation (26) is to mitigate the error caused by replacing  $\alpha \mathbf{H}^T \mathbf{n}$  with  $\alpha \sigma_n \mathbf{H}^T \mathbf{1}$  in (24). At the initial EP iteration, in (26), trainable parameters  $\mathbf{W}_0 \in \mathbb{R}^{2 \times N_u}$  and  $\mathbf{B}_0 \in \mathbb{R}^{2N_t \times N_u}$  transform the initial 2-dimensional graph signal  $\mathbf{S}^{(0)}$  to a hidden representation  $\bar{\mathbf{S}}^{(0)}$  with size  $N_u$ . We use MLP for a Multi-Layer Perceptron (MLP). The graph convolution in (28) is applied to the input graph signal  $\tilde{\mathbf{S}}^{(t)}$  to compute the output signal  $\hat{\mathbf{S}}^{(t)}$ . The attention-based network  $\text{ATT}(\mathbf{S}^{(0)})$  learns an  $M+1$  dimensional vector containing data-dependent

Chebyshev coefficients  $\text{ATT}(\mathbf{S}^{(0)})_m$  for  $m = 0, 1, \dots, M$ . The gated recurrent unit (GRU) [25] in (29) provides a gating mechanism to integrate the output signal  $\hat{\mathbf{S}}^{(t)}$  and the cavity distribution stored in  $\mathbf{P}^{(t)}$ . The output of the GRU will be the input of the GNN module at the next EP iteration. The readout module  $R$  in (30) computes the mean and variance estimation of each  $x_i$ . Two GNN layers perform (27)-(29) two times. More explanations are given in the following two subsections.

### C. Data-dependent Graph Convolution Coefficients

In equation (5), ChebNet uses conventional Chebyshev polynomial as graph filter, which uses fixed coefficients  $w_m$ . However, this architecture is less powerful and cannot perform well on testing data. Thus, in (28), we proposed to replace the fixed  $w_m$  by data-dependent learnable attention scores  $\text{ATT}(\mathbf{S}^{(0)})_m$ . Training  $\text{ATT}(\mathbf{S}^{(0)})$ , which is a function of an instance  $\{\mathbf{y}, \mathbf{H}, \sigma_n\}$ , can improve the generalization ability of the graph convolution module.  $\text{ATT}(\mathbf{S}^{(0)})$  first computes attention score  $\alpha_i$  between the default coefficient vector  $\mathbf{1}$  with size  $M+1$  and each row of the key matrix  $\mathbf{K} \in \mathbb{R}^{2N_t \times (M+1)}$ ,

$$\alpha_i = \frac{\exp(\mathbf{K}_{i,:} \cdot \mathbf{1})}{\sum_j \exp(\mathbf{K}_{j,:} \cdot \mathbf{1})}, \text{ where } \mathbf{K} = \text{MLP}_3(\mathbf{S}^{(0)}). \quad (31)$$

The  $m$ -th column of  $\mathbf{K}$  is an embedding for the  $m$ -th coefficient. The output of  $\text{ATT}(\mathbf{S}^{(0)})$  is a weighted average of each dimension of the coefficient embedding in rows of  $\mathbf{K}$ , where the attention score  $\alpha_i$  serves as the normalized weight.

$$\text{ATT}(\mathbf{S}^{(0)}) = (\sum_i \alpha_i \mathbf{K}_{i,:})^\top. \quad (32)$$

### D. Readout Module for Graph-based Estimation

At  $t^{\text{th}}$  EP iteration ( $t < T$ ), the graph convolution-based module gives an improved estimation of the standard cavity distribution in (30). The  $\text{MLP}_2$  maps  $\hat{\mathbf{S}}^{(t+1)} \in \mathbb{R}^{2N_t \times N_u}$  to a  $2N_t$  by  $2^k$  matrix, where the  $i$ -th row gives unnormalized probabilities over the constellation set. The readout function  $R$  applies row-wise softmax normalization in (10). Then the  $i$ -th row of the output  $\mathbf{P}_G^{(t)}$  represents the graph convolution-enhanced cavity distribution  $q_G^{(t)\setminus i}(x_i) = N(\hat{a}_{i,G}^{(t)}, (\hat{b}_{i,G}^{(t)})^2)$  via (11), (12), which is used to replace the cavity distribution  $q^{(t)\setminus i}(x_i)$  in (19) to compute the posterior  $\hat{p}^{(t)}(x_i)$ , and later to update the parameters for EP in (20). At the last EP iteration ( $t = T$ ), GCEPNet output the detection  $\hat{x}_G$  with  $\mathbf{P}_G^{(T)}$  in (13).

## VII. COMPUTATIONAL COMPLEXITY ANALYSIS

This section compares the complexity of the GNN module in GCEPNet and GEPNet. Both GCEPNet and GEPNet introduce additional computations to EP, which originate from their GNN modules. In (27) and (28), GCEPNet uses the graph convolution to transform the input graph signal  $\bar{\mathbf{S}}^{(t)}$  to the output signal  $\hat{\mathbf{S}}^{(t)}$ . GEPNet uses a less efficient GNN to achieve this purpose. The spatial GNN in GEPNet specifies the feature of the edges  $e_{ij}$  as  $\epsilon_{ij} = [-\mathbf{h}_i^\top \mathbf{h}_j, \sigma^2]$ , and is characterized by the following aggregation

$$\hat{\mathbf{s}}_i^{(t)} = \sum_{j \neq i} \text{MLP}_4 \left( [\bar{\mathbf{s}}_i^{(t)}, \bar{\mathbf{s}}_j^{(t)}, \epsilon_{ij}] \right). \quad (33)$$

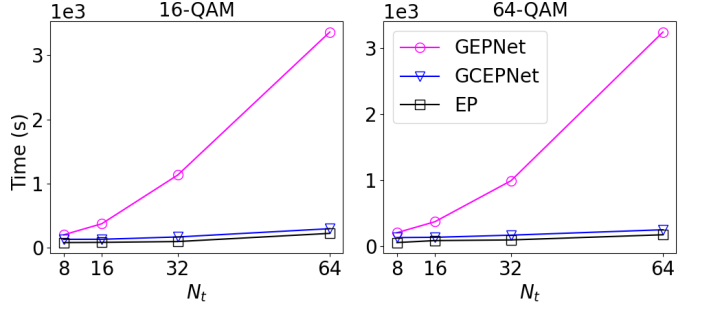


Fig. 2. The total inference running time (in seconds) for  $5 \times 10^4$  samples with  $N_t = N_r$  and the same number of EP iterations ( $T = 9$ ). Both GCEPNet and GEPNet use 2 GNN layers in each EP iteration. The implementation of GEPNet is from [16]. All methods are under CUDA acceleration.

We assume that those MLP used in GEPNet and GCEPNet all have two hidden layers with sizes  $N_{h_1}$  and  $N_{h_2}$ , to be consistent with [16]. The  $\text{MLP}_4$  in (33) has an input layer with size  $2N_u + 2$  and an output layer with size  $N_u$ . Denote  $N = 2N_t$  for simplicity, then the total cost for computing the updated hidden representations for all  $x_i$  via (33) is  $\mathcal{C}_1 = N(N-1)[(2N_u + 2)N_{h_1} + N_{h_1}N_{h_2} + N_{h_2}N_u + N_u]$ . Under the setting in [16] that  $N_u = 8$ ,  $N_{h_1} = 64$ ,  $N_{h_2} = 32$ , the coefficient of  $N^2$  is 3464 and is not negligible.

For GCEPNet, the  $\text{MLP}_1$  in (27) has an input and an output layer of size  $N_u$ , and the  $\text{MLP}_3$  in (31) has an input of size 2 and an output of size  $M+1$ , then the total cost for the graph convolution in (21), (27), (28), (31) and (32) is  $\mathcal{C}_2 = N(N_u N_{h_1} + N_{h_1} N_{h_2} + N_{h_2} N_u + N_{h_2} M + M) + N^2 N_u M$ . When  $M < 433$ ,  $\mathcal{C}_2$  has a smaller coefficient of  $N^2$  than  $\mathcal{C}_1$ . In practice, we use  $M = 3$ . Figure 2 demonstrates that, comparing with EP, GEPNet<sup>2</sup> does not scale with the problem size as a result of the inefficient GNN aggregation, while GCEPNet effectively resolves the bottleneck with the newly proposed graph convolution.

## VIII. NUMERICAL RESULTS

This section mainly compares the detection performance of GCEPNet with EP and GEPNet. GEPNet outperforms other detectors [17] except IEP-GNN [19], which has the same complexity as GEPNet. Our GNN module can be effortlessly combined with the EP module of IEP-GNN and hopefully the combined one can achieve the best performance and efficiency. But because IEP-GNN is not open-sourced, our numerical tests will not involve it. In experiments, entries of  $\mathbf{H}_c$  are generated from *i.i.d.*  $\mathcal{CN}(0, \omega_c^2)$  with  $\omega_c^2 = 1/N_r$  then get  $\mathbf{H}$ . The  $\mathbf{x}$  is uniformly sampled from  $\mathcal{X}_k^{2N_t}$  with  $\sigma_x^2 = (4^k - 1)/3$ . We find  $\sigma_n$  for the signal-to-noise ratio (SNR<sub>dB</sub>) defined by:

$$\text{SNR}_{\text{dB}} = 10 \log_{10} (\mathbb{E}\{\|\mathbf{H}_c \mathbf{x}_c\|_2^2\} / \mathbb{E}\{\|\mathbf{n}_c\|_2^2\}) \quad (34)$$

Then we generate  $\mathbf{n}$  and calculate  $\mathbf{y}$ . We use  $\{\mathbf{y}, \mathbf{H}, \sigma_n\}$  as the network input, and  $\mathbf{x}$  for computing the network loss and

<sup>2</sup>Following the implementations in [16]: <https://github.com/GNN-based-MIMO-Detection/GNN-based-MIMO-Detection>

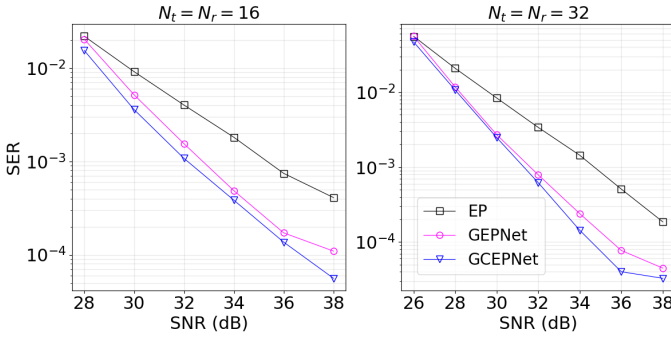


Fig. 3. The SER performance comparison for 64-QAM

the symbol error rate (SER). Let  $\mathbf{Z} \in \mathbb{R}^{2N_t \times 2^k}$  be the label matrix with  $\mathbf{Z}(i, c) = 1$  if  $x_i = \mathcal{X}_k(c)$  and 0 otherwise, the sample loss is defined as:

$$\mathcal{L} = -\text{trace}(\mathbf{Z}^\top \ln \mathbf{P}_G^{(T)}). \quad (35)$$

The training uses 850 epochs to optimize parameters in each network to minimize the average sample loss. There are 100 iterations per epoch and each iteration contains 100 training samples. Every training sample has a  $\text{SNR}_{\text{dB}}$  uniformly sampled from  $[25, 50]$ . In each epoch, the network is tested on a validation set containing 2000 samples for each  $\text{SNR}_{\text{dB}}$  from  $\{25, 26, \dots, 50\}$ . The training uses the Adam optimizer with a learning rate of  $10^{-3}$ , which is adjusted every 100 epochs according to the validation loss by the ReduceLROnPlateau scheduler in PyTorch. The network with the best mean SER on the validation set is selected for the testing stage. All networks are trained for each problem size and QAM configuration.

The testing uses  $10^5$  samples for each  $\text{SNR}_{\text{dB}}$ . Figure 3 compares the average SER of GCEPNet, GEPNet [16] and EP [9] for  $N_t = N_r = 16$  and  $N_t = N_r = 32$  with 64-QAM. Both GCEPNet and GEPNet enhance the performance of EP by incorporating correlation information into the standard cavity estimation. While GCEPNet is significantly more efficient than GEPNet, it consistently outperforms GEPNet as well. Given that GEPNet achieves the best performance among existing sub-optimal detectors [17], GCEPNet is established as the new state-of-the-art (SOTA) method.

## IX. CONCLUSION

We have proposed GCEPNet, a graph convolution-enhanced expectation propagation detector. Our analysis and numerical tests have demonstrated that GCEPNet significantly improves the efficiency of the state-of-the-art GNN-based counterparts, and consistently outperforms the existing detectors.

## REFERENCES

- [1] T. L. Marzetta, E. G. Larsson, H. Yang, and H. Q. Ngo, *Fundamentals of Massive MIMO*. Cambridge University Press, 2016.
- [2] S. Verdú, “Computational complexity of optimum multiuser detection,” *Algorithmica*, vol. 4, no. 1, pp. 303–312, 1989.
- [3] N. T. Nguyen, K. Lee, and H. DaiIEEE, “Application of deep learning to sphere decoding for large MIMO systems,” *IEEE Transactions on Wireless Communications*, vol. 20, no. 10, pp. 6787–6803, 2021.
- [4] L. V. Nguyen, N. T. Nguyen, N. H. Tran, M. Juntti, A. L. Swindlehurst, and D. H. N. Nguyen, “Leveraging deep neural networks for massive MIMO data detection,” *IEEE Wireless Communications*, pp. 1–7, 2022.
- [5] L. Bai, J. Choi, and Q. Yu, *Low Complexity MIMO Receivers*. Cham, Germany: Springer, 2014.
- [6] X.-W. Chang, Z. Chen, and J. Wen, “An extended Babai method for estimating linear model based integer parameters,” *ECONOMETRICS AND STATISTICS*, 2022.
- [7] J. Wen and X.-W. Chang, “Success probability of the Babai estimators for box-constrained integer linear models,” *IEEE Trans. Inf. Theory*, vol. 63, pp. 631–648, 2017.
- [8] X.-W. Chang, Z. Chen, and Y. Xu, “On the randomized Babai point,” in *IEEE International Symposium on Information Theory*, 2020, pp. 1195–1200.
- [9] J. Cespedes, P. M. Olmos, M. Sánchez-Fernández, and F. Perez-Cruz, “Expectation propagation detection for high-order high-dimensional MIMO systems,” *IEEE Transactions on Communications*, vol. 62, no. 8, pp. 2840–2849, 2014.
- [10] D. L. Donoho, A. Maleki, and A. Montanari, “Message-passing algorithms for compressed sensing,” *Proceedings of the National Academy of Sciences*, vol. 106, no. 45, pp. 18914–18919, 2009.
- [11] A. Scotti, N. N. Moghadam, D. Liu, K. Gafvert, and J. Huang, “Graph neural networks for massive MIMO detection,” *arXiv preprint arXiv:2007.05703*, 2020.
- [12] K. Pratik, B. D. Rao, and M. Welling, “RE-MIMO: Recurrent and permutation equivariant neural MIMO detection,” *IEEE Transactions on Signal Processing*, vol. 69, pp. 459–473, 2020.
- [13] H. He, C.-K. Wen, S. Jin, and G. Y. Li, “A model-driven deep learning network for MIMO detection,” in *2018 IEEE Global Conference on Signal and Information Processing (GlobalSIP)*. IEEE, 2018, pp. 584–588.
- [14] N. Samuel, T. Diskin, and A. Wiesel, “Learning to detect,” *IEEE Transactions on Signal Processing*, vol. 67, no. 10, pp. 2554–2564, 2019.
- [15] N. T. Nguyen and K. Lee, “Deep learning-aided tabu search detection for large MIMO systems,” *IEEE Transactions on Wireless Communications*, vol. 19, no. 6, pp. 4262–4275, 2020.
- [16] A. Kosasih, V. Onasis, W. Hardjawana, V. Miloslavskaya, V. Andrean, J.-S. Leu, and B. Vucetic, “Graph neural network aided expectation propagation detector for MU-MIMO systems,” in *2022 IEEE Wireless Communications and Networking Conference (WCNC)*. IEEE, 2022, pp. 1212–1217.
- [17] A. Kosasih, V. Onasis, V. Miloslavskaya, W. Hardjawana, V. Andrean, and B. Vucetic, “Graph neural network aided MU-MIMO detectors,” *IEEE Journal on Selected Areas in Communications*, vol. 40, no. 9, pp. 2540–2555, 2022.
- [18] H. He, A. Kosasih, X. Yu, J. Zhang, S. Song, W. Hardjawana, and K. B. Letaief, “GNN-enhanced approximate message passing for massive/ultra-massive MIMO detection,” in *2023 IEEE Wireless Communications and Networking Conference (WCNC)*. IEEE, 2023, pp. 1–6.
- [19] Z. Liu, D. He, N. Wu, Q. Yan, and Y. Li, “Model-driven IEP-GNN framework for MIMO detection with bayesian optimization,” *IEEE Wireless Communications Letters*, 2023.
- [20] A. Kosasih, V. Miloslavskaya, W. Hardjawana, C. She, C.-K. Wen, and B. Vucetic, “A bayesian receiver with improved complexity-reliability trade-off in massive MIMO systems,” *IEEE Transactions on Communications*, vol. 69, no. 9, pp. 6251–6266, 2021.
- [21] M. Defferrard, X. Bresson, and P. Vandergheynst, “Convolutional neural networks on graphs with fast localized spectral filtering,” in *Proceedings of the 30th International Conference on Neural Information Processing Systems*, 2016.
- [22] S. Luan, C. Hua, Q. Lu, J. Zhu, M. Zhao, S. Zhang, X.-W. Chang, and D. Precup, “Revisiting heterophily for graph neural networks,” *Advances in neural information processing systems*, vol. 35, pp. 1362–1375, 2022.
- [23] Q. Lu, J. Zhu, S. Luan, and X.-W. Chang, “Representation learning on heterophilic graph with directional neighborhood attention,” *arXiv preprint arXiv:2403.01475*, 2024.
- [24] S. Luan, M. Zhao, X.-W. Chang, and D. Precup, “Break the ceiling: Stronger multi-scale deep graph convolutional networks,” *Advances in neural information processing systems*, vol. 32, 2019.
- [25] K. Cho, B. Van Merriënboer, C. Gulcehre, D. Bahdanau, F. Bougares, H. Schwenk, and Y. Bengio, “Learning phrase representations using RNN encoder-decoder for statistical machine translation,” *arXiv preprint arXiv:1406.1078*, 2014.